Published in final edited form as:
*J Am Chem Soc*. 2012 June 20; 134(24): 9856–9859. doi:10.1021/ja3023785.

# Quantitative Imaging of Ion Transport through Single Nanopores by High-Resolution Scanning Electrochemical Microscopy

**Mei Shen**, **Ryoichi Ishimatsu**[†], **Jiyeon Kim**, and **Shigeru Amemiya**[*]
Department of Chemistry, University of Pittsburgh, Pittsburgh, Pennsylvania 15260

## Abstract

Here, we report on the unprecedentedly high-resolution imaging of ion transport through single nanopores by scanning electrochemical microscopy (SECM). The quantitative SECM image of single nanopores allows for the determination of their structural properties, including their density, shape, and size, which are essential for understanding the permeability of the entire nanoporous membrane. Nanoscale spatial resolution was achieved by scanning a 17 nm-radius pipet tip at a distance down to 1.3 nm from a highly porous nanocrystalline silicon membrane in order to obtain the peak current response controlled by the nanopore-mediated diffusional transport of tetrabutylammonium to the nanopipet-supported liquid/liquid interface. A 280 nm × 500 nm image resolved 13 nanopores, which corresponds to a high density of 93 pores/μm$^2$. A finite element simulation of the SECM image was performed to quantitatively assess the spatial resolution limited by the tip diameter in resolving two adjacent pores, and to determine the actual size of a nanopore, which was approximated as an elliptic cylinder with a depth of 30 nm and major and minor axes of 53 and 41 nm, respectively. These structural parameters are consistent with those determined by TEM, which thereby confirms the reliability of quantitative SECM imaging at the nanoscale level.

The development and application of nanoporous membranes for nanofiltration,[1] biomedical devices,[2] nanofluidics,[3] and biomimetic membrane transport[4] require the quantitative understanding of membrane permeability at a single nanopore level. In fact, it has been theoretically and experimentally demonstrated that the permeability of the whole nanoporous membrane depends on the convolution of several structural properties of nanopores, including their density, shape, and size.[5] Here, we applied scanning electrochemical microscopy[6] (SECM) to quantitatively and separately determine these key structural parameters from the high-resolution image of ion transport through single nanopores. Remarkably, the spatial resolution of SECM achieved in this study is the highest reported to date, with the exception of one study,[7] where no quantitative image analysis was shown.

The unprecedentedly high spatial resolution of SECM is required for the imaging of a highly porous nanocrystalline silicon (pnc-Si) membrane[8] at a single nanopore level. This emerging class of ultrathin nanoporous membranes, with a thickness of 30 nm, is robust enough to be self-standing in the aqueous solution and found to be useful for unique practical applications that require its high permeability, such as for the efficient separation of macromolecules[8a–c] and nanoparticles,[8d] tissue engineering, and cell culture.[8e] Single-pore imaging, however,

**Corresponding Author**, amemiya@pitt.edu.
[†]**Present Addresses**, Department of Applied Chemistry, Graduate School of Engineering, Kyushu University, Nishi-Ku, Fukuoka 819-0395, Japan

**ASSOCIATED CONTENT**
**Supporting Information.** This material is available free of charge via the Internet at http://pubs.acs.org.

has not been reported for a pnc-Si membrane, which not only possesses small nanopores, but also has a high pore density with short pore–pore separations of < 100 nm. Indeed, its density of ~$10^2$ pores/μm$^2$ (Figure 1A) is $10^2$–$10^6$ times higher than that of the nanopore membranes (mainly track-etched polymer membranes) that were used for the electrochemical imaging of single pores by SECM,[9] scanning ion-conductance microscopy (SICM),[10] SECM-SICM,[11] and SECM-AFM.[12] In these previous imaging studies, the shortest separations between two resolvable pores were limited to > 250 nm and ~1.5 μm for SECM(–AFM)[12b] and SICM,[10f] respectively. On the other hand, micrometer-sized SECM tips were used to probe the local permeability of a pnc-Si membrane based on several thousands of nanopores.[5b,5c]

In this work, nanoscale spatial resolution of a pnc-Si membrane was achieved by scanning a small SECM tip with a radius of 17 nm at an exceptionally short distance down to 1.3 nm. In the nanoscale SECM imaging, the current response at the nanotip is based on diffusion-controlled ion transfer at the interface between two immiscible electrolyte solutions (ITIES), which is supported at the tip of the quartz nanopipet filled with an organic electrolyte solution[13] (Figure 1B). The ionic tip current is suppressed when the tip is positioned within a tip diameter from the impermeable region of a pnc-Si membrane, which hinders ion diffusion to the nanoscale ITIES tip (i.e., negative feedback effect).[6] In contrast, the tip current increases as the tip is laterally scanned over a nanopore, which mediates ion diffusion to the ITIES tip. Subsequently, a peak-shaped response is obtained during a line scan over a pore (Figure 1B), where a shorter tip–membrane distance enhances the image contrast based on the peak height and improves spatial resolution based on the peak width.[6]

A nanopipet-based SECM tip was prepared as reported elsewhere[13b] and characterized by ion-transfer voltammetry and SEM. A nanopipet was filled with the 1,2-dichloroethane solution of organic supporting electrolytes and immersed in an aqueous solution of tetrabutylammonium (TBA) in order to voltammetrically drive TBA transfer across the nanopipet-supported ITIES (Figure 2A). The sigmoidal steady-state voltammograms on forward and reverse potential sweeps show small capacitive current and nearly overlap with each other. The pipet-supported ITIES tip was assumed as an inlaid disk, and therefore a limiting current, $i_{T,\infty}$, of 42 pA corresponds to a tip inner radius, $a$, of 17 nm with a typical tip outer radius, $r_g$, of 1.4$a$ as determined from

$$i_{T,\infty} = 4xnFDc^*a \quad (1)$$

where $x$ is a function of $RG$ (= $r_g/a$),[16] $n$ is the number of transferred charges (= +1) in the tip reaction, and $D$ (= 5.1 × $10^{-6}$ cm$^2$/s) and $c^*$ (= 10 mM) are the diffusion coefficient and concentration of the transferred ion in the bulk solution, respectively. The inner radius of the ITIES tip is similar to that of a typical nanopipet (~15 nm) as estimated by SEM (Figure 2B).

The nanopipet-supported ITIES tip was employed for the imaging of a pnc-Si membrane using the constant-height mode of SECM[6] (i.e., without the active feedback control of the tip−membrane distance) in a newly developed isothermal chamber, which supresses a distance change due to thermal drift to a subnanometer level.[13b] In addition, the flat surface of the pnc-Si membrane with a root-mean-square roughness of 0.29 nm as measured by AFM[14] was horizontally aligned on the SECM stage using a bubble level[15] to be perpendicular to the tip electrode axis. Subsequently, we observed that a sharp nanopipet with small $RG$ of 1.4 approached very closely to the flat substrate and was scanned laterally without contact when a relatively small area of the membrane was imaged (see below; also Figure S-1 for details).

The whole procedure for obtaining an SECM image (Figure 3A) is illustrated in Figure 3B using the corresponding time profile of the current response at the nanopipet-supported ITIES tip. Prior to imaging, the tip was brought in close proximity to a pnc-Si membrane and stopped when the tip current decreased to 40% of $i_{T,\infty}$ (Figure 3B). In this example, the tip approached pore **1** at ($x$, $y$) = (0, 0) (Figure 3A). The tip then remained over the pore for 35 s until the tip was scanned from $x$ = 0 nm to $x$ = 280 nm with a step size of 4 nm, which was repeated from $y$ = 0 nm to $y$ = 500 nm with an interval of 5 nm. It took approximately 0.1 s at each tip position to move and settle the $x$, $y$-axes piezo positioner and monitor the steady-state tip current.

During the 280 nm × 500 nm scan (Figure 3A), the height of a peak current response to a pore under the tip varied with a lateral distance between tip and pore, thereby yielding a family of peaks with various heights for each nanopore (Figure 3B). In contrast, the negative feedback current at the foot of a current peak was very stable and reproducible, which confirmed that the tip–membrane distance was nearly constant during imaging. A tip current, $i_T$, of 10 pA in Figure 3B is equivalent to a tip–membrane distance of 1.3 nm in the approximate equation with $RG$ = 1.4.[13b] A stable distance was also maintained between the tip and pore **13** to give a constant current after the imaging was completed. Finally, the tip current nearly recovered to the initial $i_{T,\infty}$ value when the tip was withdrawn to 1.5 μm away from the substrate. The good stability of the tip current indicates a lack of significant tip damage due to tip–membrane contact during imaging.

Overall, 13 pores were successfully resolved as local regions with higher tip currents in the SECM image of a pnc-Si membrane (Figure 3A). This result corresponds to a high density of 93 pores/μm$^2$, which is consistent with a density of ~90 pores/μm$^2$, as determined from the TEM image (Figure 1A). Qualitatively, a larger pore occupies a larger area in the SECM image, where pores **9, 10**, and **11** are significantly smaller than the other pores. The area occupied by a pore in the image, however, is larger than expected from the actual size of the pore, because the spatial resolution is limited by the tip size that is comparable to the pore size. Therefore, the quantitative analysis of the SECM image is needed to reliably evaluate pore size (see below). Noticeably, unidirectional orientation is seen for some pores in the SECM image, which may be due to the imperfect disk shape of the ITIES supported at an elongated tip orifice. We found that the orientation of nanopores varied from tip to tip, but was independent of the tip−membrane distance (1.3–8.5 nm), and was different from the direction of the tip scan (Figure 3A).

SECM line scans over pore **7** were analyzed by employing the finite element simulation of ion diffusion around the tip and the nanopore (see Supporting Information) to reliably determine the actual pore size without the limitation of spatial resolution set by the tip size (Figure 4). For simplicity, the $x$, $y$-cross section of a pore was assumed to be elliptical in shape, thereby yielding the major and minor axes and depth of a pore as structural parameters. TBA is small enough to freely diffuse through a nanopore without electrostatic or steric hindrance from the pore wall.[5c] Figure 4A shows very good fits of simulation results with experimental results, where each peak current response in a $x$ line scan was plotted against the $x$ position of the center of the tip with respect to that of the center of each nanopore, i.e., $\Delta x$, while $\Delta y$ represents the corresponding relative $y$ position of the tip (see also Figure S-3 for these definitions). The simulation results show that pore **7** has major and minor axes of 53 nm and 41 nm, respectively. An aspect ratio of 1.3 is consistent with the corresponding values of 1.0–2.1, as determined from ~150 pores in the TEM image (Figure 1A). Moreover, the average of the major and minor axes gives an apparent pore diameter[5b] of 47 nm, which is in agreement with the corresponding values of 14–58 nm in the TEM image. Moreover, the apparent diameter determined by numerical simulation is much smaller than an apparent pore diameter of ~80 nm for pore **7**, as determined from its SECM

image, where major and minor axes of ~90 and ~70 nm, respectively, were obtained from the area surrounded by a contour line of ~11 pA. Noticeably, a pore depth of 30 nm was also confirmed by the simulation of peak currents in Figure 4A, which are sensitive to the pore depth (see Figure S-4).

The simulated concentration profiles of TBA around pore **7** during the $x$-line scan at $\Delta y = 0$ nm are shown in parts B–D of Figure 4 to quantitatively demonstrate how the tip size limits spatial resolution in determining acture pore size and separating two adjacent nanopores. In Figure 4B, the center of the tip is positioned by approximately a tip radius away from the edge of the pore, and thus the whole tip surface is positioned above the impermeable region of the membrane. The resultant negative feedback current determines the base of a current peak (red dot 1 in Figure 4A). Therefore, the apparent pore size estimated from the current peak (or the SECM image) is larger than the actual pore size by a tip inner diameter of 34 nm, which is confirmed for pore **7** with apparent diameters of ~80 and 47 nm, as determined from the SECM image and its simulation, respectively (see above). In fact, when the center of the tip is positioned above the edge of the nanopore (Figure 4C), the corresponding tip current (red dot 2) is significantly enhanced by ion diffusion from the inside of the pore and already reaches more than half of the peak current (red dot 3) that is obtained when the tip center is positioned above the center of the nanopore (Figure 4D). These results also indicate that two adjacent nanopores can be completely separated in the SECM image only when their edge-edge separation is larger than the tip inner diameter. For instance, pore **8** partially overlaps with pore **9** in Figure 3A, because their center-center separation of only ~55 nm is comparable to a typical pore diamater.

In summary, SECM was successfully used to generate the unprecedented high-resolution and quantitative imaging of single nanopores at a high density of 93 pores/$\mu m^2$. The SECM image can be quantitatively analyzed to determine the structural properties of single nanopores, including the smallest pore axis of 41 nm, without the limitation of spatial resolution set by the tip diameter. The numerical simulation also indicates that two adjacent pores with an edge-edge separation of the tip diameter or larger, i.e., ≥ 34 nm in this work are completely resolvable. Advantageously, the highest resolution of SECM under normal experimental conditions was achieved in this study by employing the simple constant-height mode without feedback distance control, not only because the pnc-Si membrane surface was flat, but also because the SECM stage was isolated from the ambient environment using an isothermal chamber to suppress thermal drift.[13b] Based on these findings, we envision the application of this simple, quantitative, and high-resolution SECM approach to the imaging of biological nanopores.[17]

## Supplementary Material

Refer to Web version on PubMed Central for supplementary material.

## Acknowledgments

This work was supported by grants from the National Institutes of Health (GM073439). We thank Dr. Christopher C. Striemer and Mr. Charles Chan, SiMPore, for the TEM images of pnc-Si membranes and their analysis.

## REFERENCES

1. (a) Vandezande P, Gevers LEM, Vankelecom IFJ. Chem. Soc. Rev. 2008; 37:365. [PubMed: 18197351] (b) Shannon MA, Bohn PW, Elimelech M, Georgiadis JG, Marinas BJ, Mayes AM. Nature. 2008; 452:301. [PubMed: 18354474] (c) Peng XS, Jin J, Nakamura Y, Ohno T, Ichinose I. Nat. Nanotechnol. 2009; 4:353. [PubMed: 19498395] (d) Karan S, Samitsu S, Peng X, Kurashima K, Ichinose I. Science. 2012; 335:444. [PubMed: 22282807]

2. (a) Kooman JP, van der Sande FM, Leunissen KML. Blood Purification. 2007; 25:377. [PubMed: 17785967] (b) Fissell WH, Dubnisheva A, Eldridge AN, Fleischman AJ, Zydney AL, Roy S. J. Membr. Sci. 2009; 326:58.(c) Perin L, Da Sacco S, De Filippo RE. Adv. Drug Deliv. Rev. 2011; 63:379. [PubMed: 21145933]
3. (a) van den Berg A, Wessling M. Nature. 2007; 445:726. [PubMed: 17301783] (b) Schoch RB, Han JY, Renaud P. Rev. Mod. Phys. 2008; 80:839.(c) Li YQ, Zheng YB, Zare RN. ACS Nano. 2012; 6:993. [PubMed: 22304827]
4. (a) Jovanovic-Talisman T, Tetenbaum-Novatt J, McKenney AS, Zilman A, Peters R, Rout MP, Chait BT. Nature. 2009; 457:1023. [PubMed: 19098896] (b) Kowalczyk SW, Kapinos L, Blosser TR, Magalhaes T, van Nies P, Lim RYH, Dekker C. Nat. Nanotechnol. 2011; 6:433. [PubMed: 21685911]
5. (a) Berg, HC. Random Walks in Biology. Princeton, NJ: Princeton University Press; 1993. (b) Kim E, Xiong H, Striemer CC, Fang DZ, Fauchet PM, McGrath JL, Amemiya S. J. Am. Chem. Soc. 2008; 130:4230. [PubMed: 18324815] (c) Ishimatsu R, Kim J, Jing P, Striemer CC, Fang DZ, Fauchet PM, McGrath JL, Amemiya S. Anal. Chem. 2010; 82:7127. [PubMed: 20690617]
6. (a) Bard, AJ.; Mirkin, MV., editors. Scanning Electrochemical Microscopy. New York: Marcel Dekker; 2001. (b) Amemiya S, Bard AJ, Fan FRF, Mirkin MV, Unwin PR. Ann. Rev. Anal. Chem. 2008; 1:95.
7. Fan FRF, Bard AJ. Proc. Natl. Acad. Soci. U.S.A. 1999; 96:14222.
8. (a) Striemer CC, Gaborski TR, McGrath JL, Fauchet PM. Nature. 2007; 445:749. [PubMed: 17301789] (b) Fang DZ, Striemer CC, Gaborski TR, McGrath JL, Fauchet PM. Nano Lett. 2010; 10:3904. [PubMed: 20839831] (c) Snyder JL, Clark A, Fang DZ, Gaborski TR, Striemer CC, Fauchet PM, McGrath JL. J. Membrane Sci. 2011; 369:119.(d) Gaborski TR, Snyder JL, Striemer CC, Fang DZ, Hoffman M, Fauchet PM, McGrath JL. ACS Nano. 2010; 4:6973. [PubMed: 21043434] (e) Agrawal AA, Nehilla BJ, Reisig KV, Gaborski TR, Fang DZ, Striemer CC, Fauchet PM, McGrath JL. Biomaterials. 2010; 31:5408. [PubMed: 20398927]
9. (a) Bath, BD.; White, HS.; Scott, ER. Scanning Electrochemical Microscopy. Bard, AJ.; Mirkin, MV., editors. New York: Marcel Dekker; 2001. p. 343(b) Uitto OD, White HS. Anal. Chem. 2001; 73:533. [PubMed: 11217758] (c) Uitto OD, White HS, Aoki K. Anal. Chem. 2002; 74:4577. [PubMed: 12236372] (d) Lee S, Zhang Y, White HS, Harrell CC, Martin CR. Anal. Chem. 2004; 76:6108. [PubMed: 15481960] (e) Ervin EN, White HS, Baker LA. Anal. Chem. 2005; 77:5564. [PubMed: 16131066] (f) Ervin EN, White HS, Baker LA, Martin CR. Anal. Chem. 2006; 78:6535. [PubMed: 16970331] (g) White RJ, White HS. Anal. Chem. 2007; 79:6334. [PubMed: 17640104] (h) McKelvey K, Snowden ME, Peruffo M, Unwin PR. Anal. Chem. 2011; 83:6447. [PubMed: 21776952]
10. (a) Proksch R, Lal R, Hansma PK, Morse D, Stucky G. Biophys. J. 1996; 71:2155. [PubMed: 8889191] (b) Böcker M, Muschter S, Schmitt EK, Steinem C, Schäffer TE. Langmuir. 2009; 25:3022. [PubMed: 19437710] (c) Chen C-C, Derylo MA, Baker LA. Anal. Chem. 2009; 81:4742. [PubMed: 19435340] (d) Chen -CC, Baker LA. Analyst. 2011:136.(e) Chen C-C, Zhou Y, Baker LA. ACS Nano. 2011; 5:8404. [PubMed: 21923184] (f) Zhou Y, Chen CC, Baker LA. Anal. Chem. 2012; 84:3003. [PubMed: 22390616]
11. (a) Takahashi Y, Shevchuk AI, Novak P, Zhang Y, Ebejer N, Macpherson JV, Unwin PR, Pollard AJ, Roy D, Clifford CA, Shiku H, Matsue T, Klenerman D, Korchev YE. Angew. Chem. Int. Ed. 2011; 50:9638.(b) Morris CA, Chen C-C, Baker LA. Analyst. 2012 Advance Article, http://dx.doi.org/10.1039/C2AN16178H.
12. (a) Macpherson JV, Unwin PR. Anal. Chem. 2000; 72:276. [PubMed: 10658320] (b) Macpherson JV, Jones CE, Barker AL, Unwin PR. Anal. Chem. 2002; 74:1841. [PubMed: 11985316] (c) Gardner CE, Unwin PR, Macpherson JV. Electrochem. Comm. 2005; 7:612.
13. (a) Elsamadisi P, Wang Y, Velmurugan J, Mirkin MV. Anal. Chem. 2011; 83:671. [PubMed: 21162580] (b) Kim J, Shen M, Nioradze N, Amemiya S. Anal. Chem. 2012; 84:3489. [PubMed: 22462610]
14. Fang, DZ. Ph.D. Dissertation. University of Rochester: Rochester, NY; 2010.
15. Sun P, Mirkin MV. Anal. Chem. 2006; 78:6526. [PubMed: 16970330]
16. Lefrou C. J. Electroanal. Chem. 2006; 592:103.
17. Guo J, Amemiya S. Anal. Chem. 2005; 77:2147. [PubMed: 15801749]

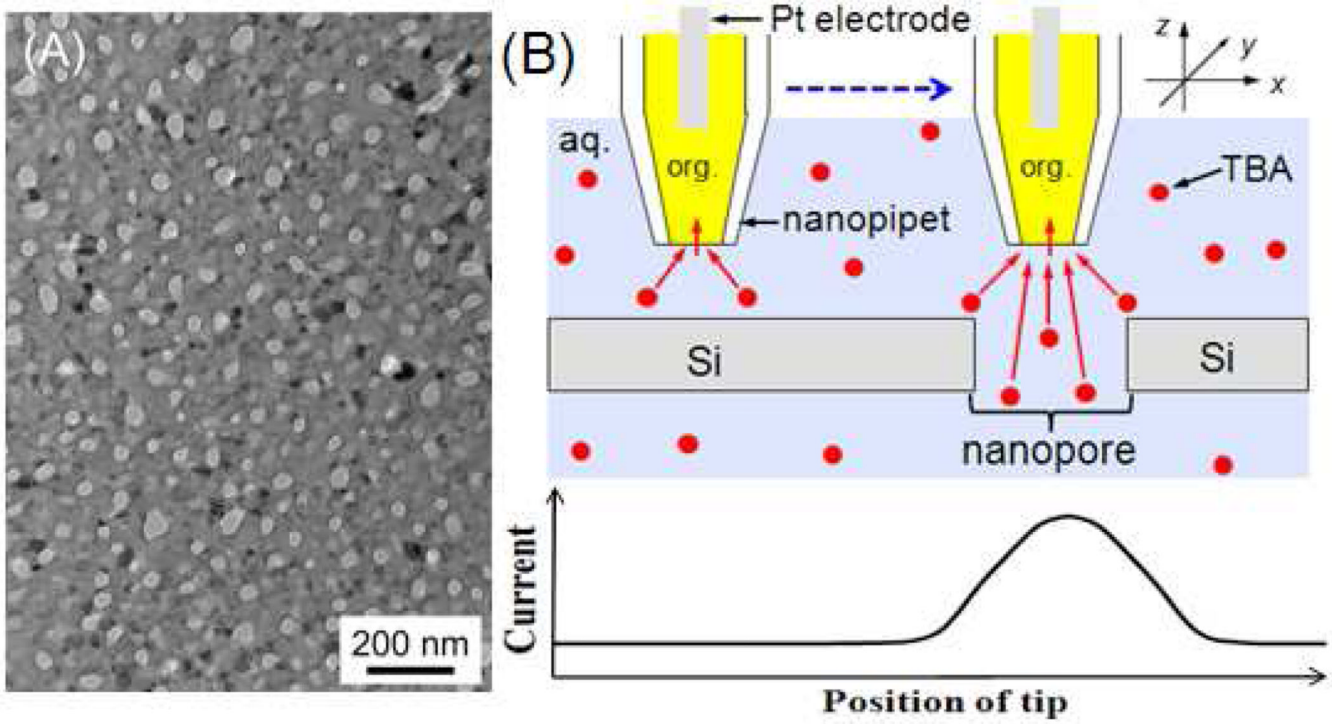


**Figure 1.**
(A) TEM image of a pnc-Si membrane and (B) scheme of SECM line scan with a nanopipet-supported ITIES tip over the impermeable and nanoporous regions of the membrane.

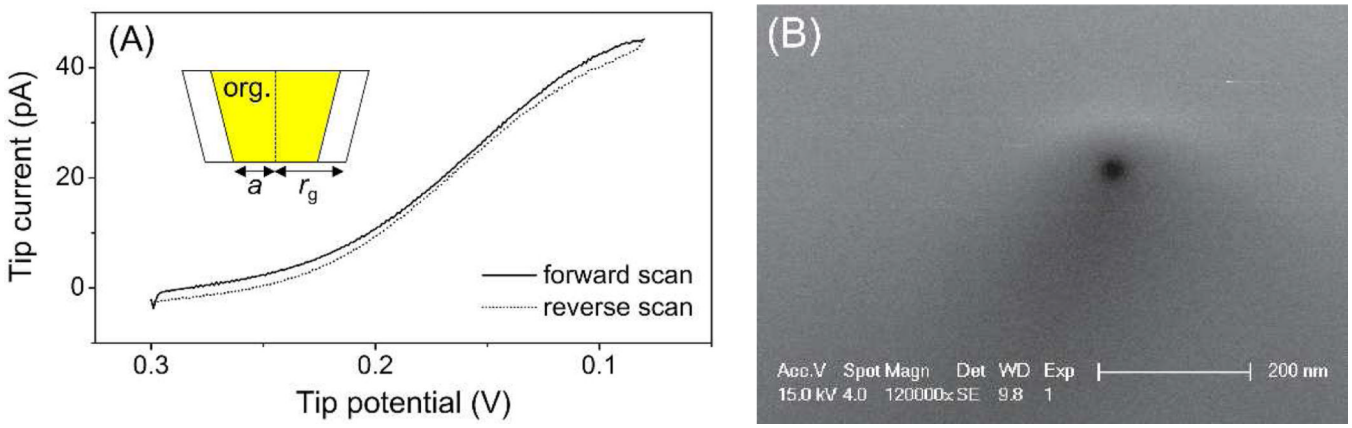


**Figure 2.**

(A) Cyclic voltammetry of 10 mM TBA in 0.3 M KCl at 50 mV/s. The tip potential is defined against an Ag/AgCl reference electrode. (B) SEM image of the tip opening of a typical nanopipet.

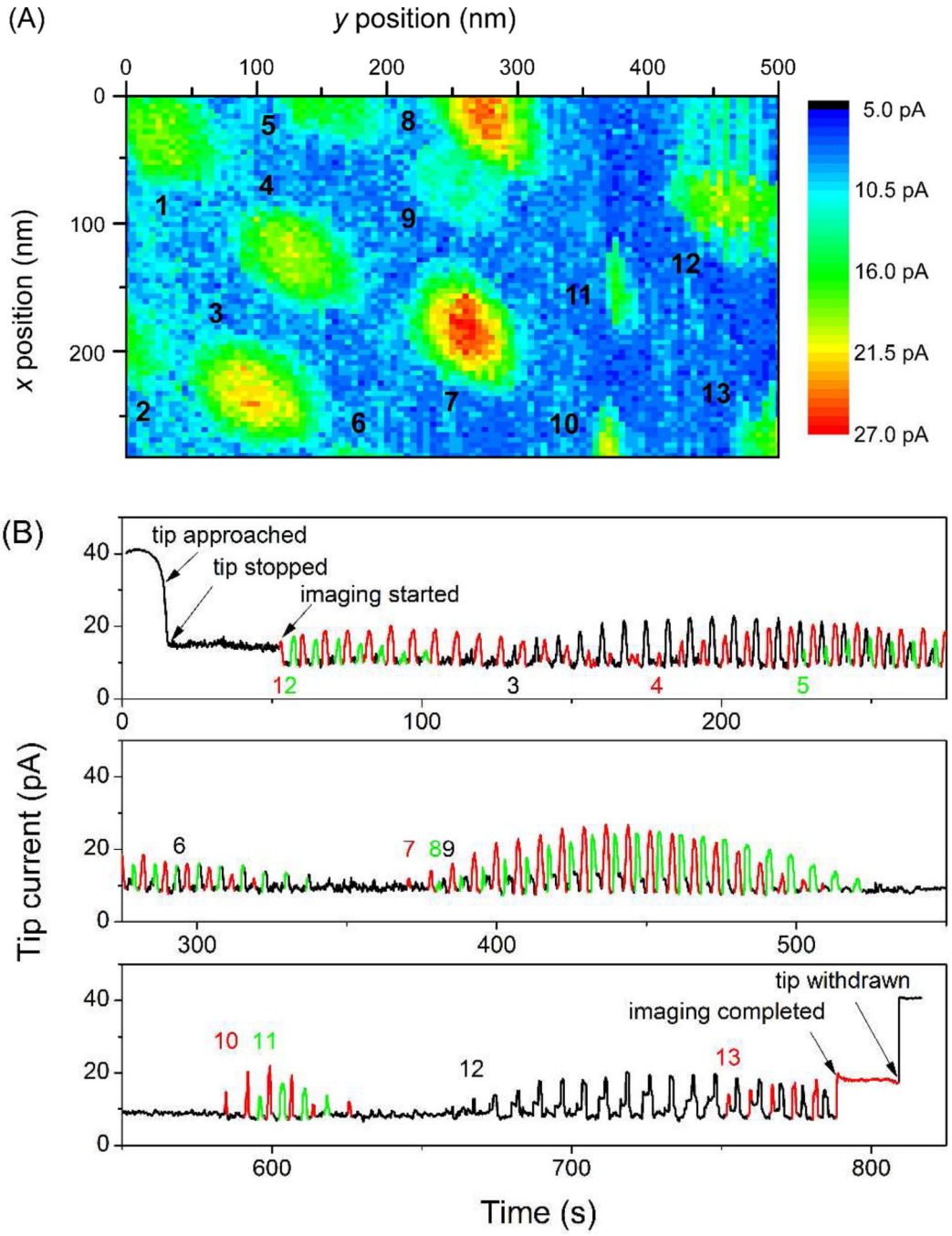


**Figure 3.**
(A) SECM image of a pnc-Si membrane and (B) current versus time profile during the whole imaging experiment, where a number is given for each pore at the time when its first peak appears.

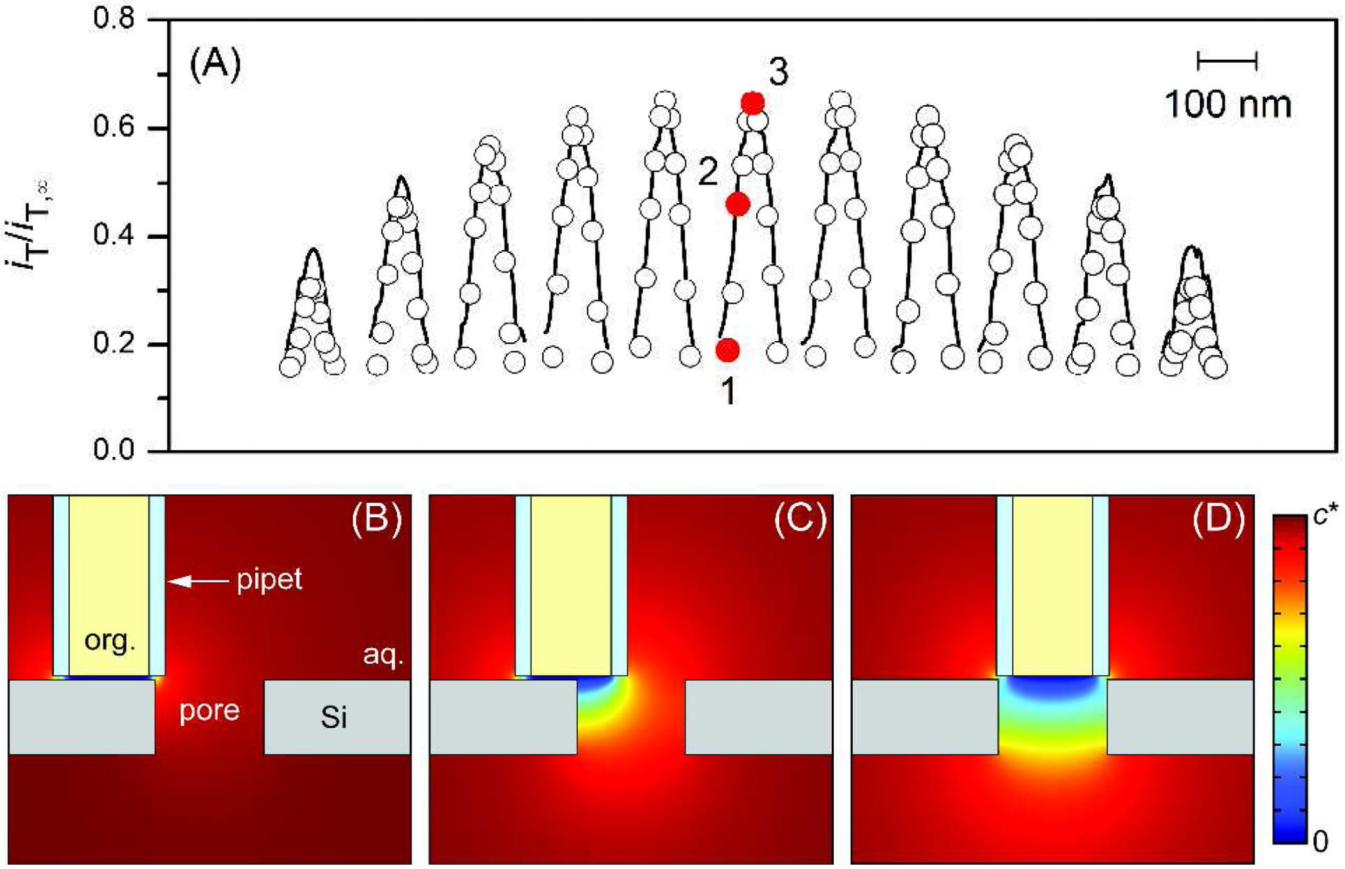


**Figure 4.**

(A) Simulated (circles) and experimental (solid lines) tip current, $i_T/i_{T,\infty}$, in the normalized form for *x*-line scans over pore **7**. In the simulation, the *y* position of the tip center was kept at $\Delta y = -35, -25, -15, -10, -5, 0, +5, +10, +15, +25$, and +35 nm from the leftmost peak to the rightmost peak, while its *x* position for each line scan was $\Delta x = -42.5, -34, -25.5, -17, -8.5, 0, +8.5, +17, +25.5, +34$, and +42.5 nm from the leftmost circle to the rightmost circle. Sliced concentration profiles are shown for tip positions at $\Delta x =$ (B) −42.5, (C) −25.5, and (D) 0 nm and $\Delta y = 0$ nm, as indicated by red dots 1–3, respectively, in part (A).